

LASER PULSE SHAPING FOR GENERATION OF LOW-EMITTANCE ELECTRON-BEAM

Changbum Kim, Jaehun Park, PAL, POSTECH, Pohang 790-784

Kiho Hyun, Chang-Mook Yim, Yong Woon Parc, and In Soo Ko, POSTECH, Pohang 790-784

Abstract

A photocathode RF gun can provide a high-charge short-bunch-length electron beam, so that it can be used for an injector of the 4th generation light source. However, owing to the high-charge in short-bunch-length, generated electron beam experiences severe space-charge effect in the beginning of acceleration and the emittance becomes bad rapidly. To reduce this space-charge effect, we made a preliminary study of pulse shaping technique. First, Parmela simulations are performed to check the beam quality improvement when the flat-top profile laser is used. Given geometry of the photocathode RF gun in the Pohang Accelerator Laboratory, Parmela simulations show 40% decrease of the emittance in electron beams. Next, by stacking four Gaussian pulses to the longitudinal direction, we tried a generation of flat-top profile laser, and its profile is checked with a cross-correlator.

INTRODUCTION

The electron source for the X-ray FEL [1-3] requires a very-low-emittance (high brightness) electron beam as low as 1 mm-mrad [4]. Photocathode RF-gun is the reliable candidate for low emittance like this and the minimization of emittance growth in the RF-gun is needed for low emittance. In general, emittance growth occurs close to the cathode surface in the RF-gun and is caused by defocusing space-charge force and nonlinear space-charge effect. These effects can be reduced by optimizing the charge density distribution of electron-beam, where optimizing represents making the uniform charge density distribution. It is a widely known fact but we have investigated that it can be applied to our photocathode RF-gun with PARMELA code. Charge density distribution of electron-beam is decided by the laser pulse intensity distribution just before irradiation at photocathode. Thus, the laser pulse with uniform intensity distribution is needed for low-emittance electron beam generation as low as 1 mm-mrad. Several X-ray FEL projects developed the photocathode RF-gun and laser system with uniform intensity distribution [4-6]. Mostly, conventional streak cameras were used to monitor their laser pulses. In this article, we introduce a technique to make longitudinally uniform laser pulse shape and a diagnostics method of this laser pulse. This diagnostics method is based on cross-correlation measurement with nonlinear crystals. We have made a 4-pulse generator for longitudinally uniform laser pulse shaping and designed a cross-correlation system for pulse diagnostics. In addition, we introduce the existing laser system briefly.

SIMULATION

We have investigated the difference between longitudinally Gaussian electron beam and longitudinally uniform electron beam with PARMELA code, where both of them have transversely uniform distribution.

Emittance can be separated into various elements according to the causes, which are the linear space-charge induced emittance (\mathcal{E}_{sc}), the linear RF induced emittance (\mathcal{E}_{rf}), the thermal emittance (\mathcal{E}_{th}), and etc [7]. Thus, emittance can be written as,

$$\mathcal{E} = \sqrt{\mathcal{E}_{sc}^2 + \mathcal{E}_{rf}^2 + \mathcal{E}_{th}^2 + \dots} \quad (1)$$

According to the analytical models, the linear space-charge induced emittance and RF induced emittance may be described as $\mathcal{E}_{sc} \propto (Q/\sigma_z)\mu(A)$ and $\mathcal{E}_{rf} \propto \sigma_x^2\sigma_z^2$, where $\mu(A)$ is referred to the transverse space-charge factor, $A = \sigma_x/\sigma_z$, Q is the bunch charge, σ_x and σ_z represent the beam spot size and bunch length respectively. Because only \mathcal{E}_{sc} has the charge dependency, emittance can be written as,

$$\mathcal{E} = \sqrt{(aQ)^2 + b^2}, \quad (2)$$

where a is a parameter referred to the space-charge force, and b is the sum of the RF induced emittance, the thermal emittance, and etc.

Using the above theory, we have analyzed the simulation data. Figure 1 shows the normalized rms horizontal emittance as the electron bunch charge with the longitudinally Gaussian beam and longitudinally uniform beam at the position of 150 cm from the cathode, at which accelerating column will be installed. Electron bunch length (full width of half maximum, FWHM) is fixed at 10 ps to have the same RF induced emittance about both of them and the thermal emittance is independent on electron beam shape. Therefore, fitting the data as Eq. 2, we can obtain the parameter a and b with each electron beam shape, where a is referred to the space-charge force as mentioned above and b is referred to the nonlinear space-charge effect because RF induced emittance and thermal emittance are the same with both of them. The fits yield $a = 1.36 \pm 0.059$ and $b = 0.97 \pm 0.04$ in the longitudinally uniform shape, while $a = 2.11 \pm 0.059$ and $b = 1.49 \pm 0.04$ in the longitudinally Gaussian shape. From the obtained parameter a , we can find out that uniform shape reduces the space-charge force of about 40%. In addition,

comparing the parameter b with each electron beam shape, it is found that uniform shape reduces the emittance growth due to the nonlinear space-charge effect which is not removed in the solenoid emittance compensation. From this simulation analysis, we have confirmed the need of longitudinally uniform electron beam for the success of PAL-XFEL project [8].

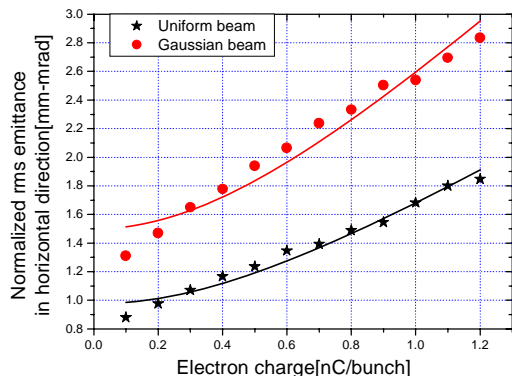


Figure 1: Normalized rms horizontal emittance vs. electron bunch charge

LONGITUDINAL LASER PULSE SHAPING

Laser System

In 2005, a Ti:Sapphire laser system (Spectra Physics) was installed for the photocathode RF-gun in a gun test stand (GTS) [9]. This laser system will be used in FIR-Linac which is being constructed now [10]. Laser system consists of an oscillator, a regenerative amplifier, a tripler for third harmonic generation (THG), and a custom designed UV stretcher (Laser Spectronix). The laser system is installed in a clean room which temperature is controlled within 0.5°C for stable operations. From the oscillator, mode locked, about 100 fs pulse width, 800 nm wavelength infrared (IR) laser pulses are generated with 80 MHz repetition rate (nominal). These laser pulses come into the regenerative amplifier, which amplifies laser pulse energy up to 2.5 mJ with 1 kHz repetition rate (nominal). Regenerative amplifier works with the chirped pulse amplification (CPA) method against the damage of gain medium. After the regenerative amplifier, the laser pulses come into a tripler which produces 266 nm wavelength ultraviolet (UV) laser pulses with THG. The UV laser pulse still has an ultra short pulse width, which stimulates high space-charge effect. So UV stretcher is installed to change the pulse width. To increase the UV pulse width, two prism pairs are used in the UV stretcher. UV pulse width is changed according to the position of the movable mirrors between two prism pairs. UV pulse width is calculated with cross-correlation measurements based on 2nd order nonlinear effect [11], where the measurement method is described detailedly later. From

this result, we can find out that UV pulse width and distance between prism pairs are linearly related.

4-Pulse Generator

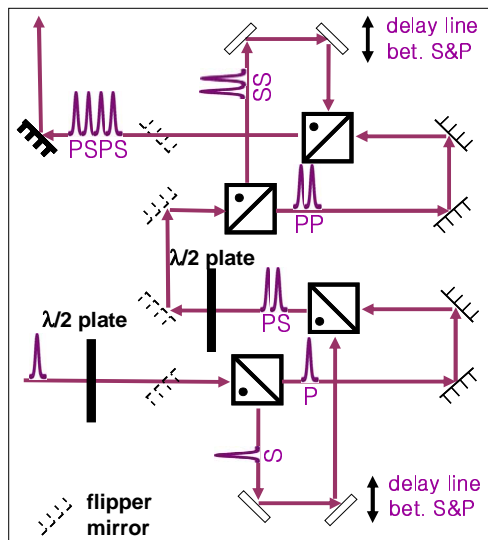


Figure 2: Layout of 4-pulse generator and timing chart

4-pulse generator

In general, the laser pulse generated from Ti:Sapphire laser system has longitudinally Gaussian shape. To change the longitudinally Gaussian shape into the longitudinally uniform shape, we have installed 4-pulse generator behind a UV stretcher. 4-pulse generator is an equipment to make the uniform pulse shape with pulse stacking method. 4-pulse generator consists of 2 stages and each stage is composed of two polarizing beam splitters (PBS), a half-wave plate, and an optical delay line. As shown in figure 2, the full s-polarization is rotated to a 45-degree polarization with a half-wave plate. It is then divided into an s-polarized pulse and a p-polarized one with the first PBS. The s-polarized pulse is delayed with an optical delay line and then combined with the p-polarized pulse after using the next PBS. After next stage with the same components, the stacked four pulses are generated. The polarized angles of micro pulses are perpendicular to each adjacent micro pulse. That prevents the interference between adjacent micro pulses. If we adjust each optical delay line as the full width of half maximum of micro pulse, we can get the macro pulse with longitudinally uniform shape. The reason for using 4 pulses but not using 8 or 16 pulses, which can make more uniform shape than 4 pulses, is related to the threshold damage of PBS used in our laser system. That is to say, assuming that the macro pulse composed of 8 or 16 micro pulses have the same pulse length with one composed of 4 micro pulses, where optimized macro pulse length is about 10 ps, 8 or 16 micro pulses have shorter pulse length than 4 micro pulses. Therefore, 4 micro pulses don't damage the PBS under this micro pulse length but 8 or 16 micro pulses may damage the PBS. In figure 2, flipper mirrors are aimed to generate one pulse or two pulses. Using these flipper mirrors, we can diagnose the each stage of 4-pulse generator.

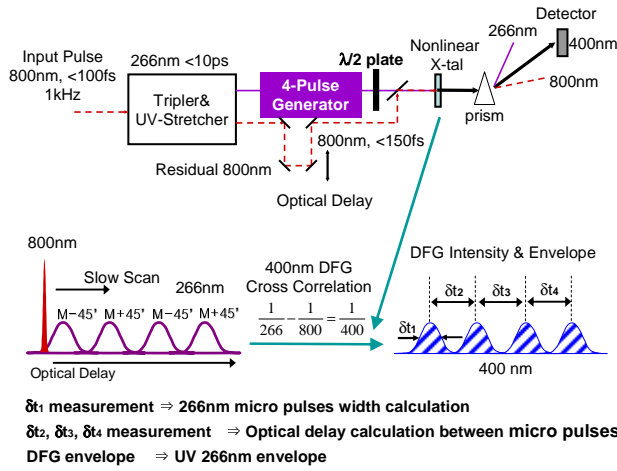


Figure 3: Layout of cross-correlation system for mixed polarizations and principles.

Cross-correlation system for mixed polarizations

Next to the 4-pulse generator, a cross-correlation system is installed to diagnose the UV pulse. This cross-correlation system is specially designed for mixed polarizations. If the stacked 266 nm and the short 800 nm lasers are overlapped in the nonlinear crystal (BBO), the 400 nm signal can be observed by the difference frequency generation (DFG). We can obtain the intensity profile of the 400 nm signal by scanning the optical delay of 800 nm laser. In the case of stacked pulses, however, each micro pulse makes different 400nm DFG intensity according to its polarized angle. We can understand this mechanism from phase matching condition in BBO nonlinear crystal. BBO crystal, which we have used, is a negative uniaxial crystal and optimized at type I phase matching. Eq. 3 represents the type 1 phase matching condition about DFG in the case of collinear rays [12].

$$n_{dfg}^e \omega_{dfg} = n_{uv}^o \omega_{uv} - n_{ir}^o \omega_{ir}, \quad (3)$$

where super script e and o represent extraordinary ray and ordinary ray respectively. From phase matching condition, it is found that only o-ray component of UV pulse makes DFG, and so different 400 nm DFG intensity occurs according to polarized angle of UV pulse. Against it, we should have UV pulses produce the same DFG intensity independent of polarized angles. As shown in figure 4, if we set each micro pulse's polarized angle into ± 45 -degree from a reference ray (o-ray) with half-wave plate behind the 4-pulse generator, we can get the same 400nm DFG intensity apart from the polarized angle of each micro pulse. Thus, we have installed a half-wave plate behind the 4-pulse generator to rotate the polarized angles. Using the cross-correlation system for mixed polarizations, we can not only measure the pulse width of a micro pulse but also diagnose the pulse shape of a macro pulse (See the bottom in figure 3)

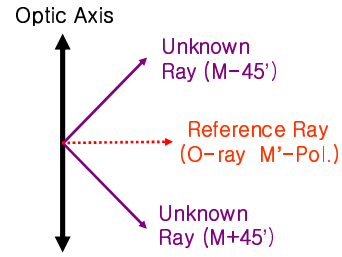


Figure 4: Polarized angle adjustment to obtain the same 400nm DFG intensity about micro pulses with different polarized angles. Unknown rays represent UV pulses.

Diagnostics of stacked pulses

As shown in Figure 5, we have measured the 400nm DFG signal under various optical delays with cross-correlation system. In Figure 5, (a) is the measurement result in the case without delays between micro pulses. (b) and (c) are the measurement results in the case with delay as FWHM and 4 sigma of micro pulse respectively. 0.53 mm means a micro pulse width of 1.76 ps and 1.29 mm means a micro pulse width of 4.30 ps, where 1.76 ps and 4.30 ps is the FWHM and 4 sigma of micro pulse respectively. As shown in the case of (b), macro pulse has longitudinally uniform intensity distribution over all. We have succeeded in longitudinally uniform laser pulse shaping. In addition, we can find out that optical delays are controlled precisely.

In general, streak camera is widely used for laser pulse diagnostics. However, it is a very expensive equipment and has poor time resolution than the cross-correlation method, which is a relatively inexpensive equipment. On the other hand, cross-correlation method is not suitable for stacked pulses with mixed polarizations. Thus, we have designed a modified cross-correlation system for mixed polarizations, in which we use half-wave plate to control the polarizations of pulses, and we obtained useful results with it.

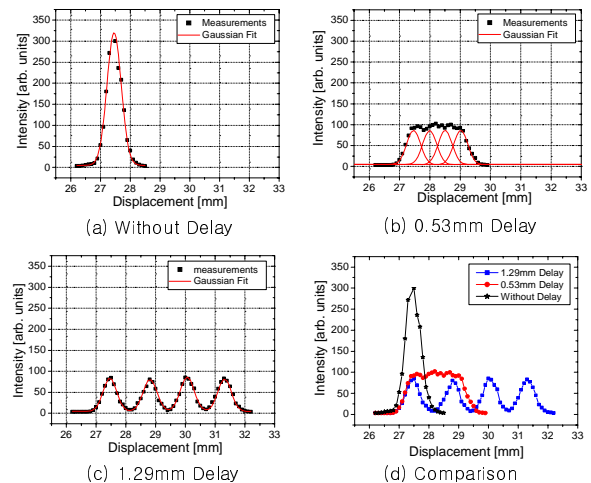


Figure 5: 400nm DFG signal measurements under various optical delays. We can obtain the intensity profile of UV pulses from this result at second hand.

SUMMARY

We have made a 4-pulse generator for longitudinally uniform laser pulse shaping and designed a cross-correlation system for mixed polarizations. We have verified the pulse stacking technique with these equipments. And we have diagnosed the stacked pulses with mixed polarizations easily and efficiently with modified cross-correlation system.

ACKNOWLEDGEMENT

The authors would like to thank H. Tomizawa (SPring-8) and J. S. Kim (Laser Spectronix Co., Ltd.) for valuable discussions. This work was supported by the Korea Science and Engineering Foundation (KOSEF) grant funded by the Korea government (MEST) (No. R01-2006-000-11309-0, R0A-2008-000-20013-0).

REFERENCES

- [1] Linac Coherent Light Source (LCLS) Conceptual Design Report, SLAC-R-593 (April 2002)
- [2] The European X-ray Free-Electron Laser Technical Design Report (July 2007)
- [3] SCSS X-FEL Conceptual Design Report, RIKEN (May 2005)
- [4] J. Yang, F. Sakai, T. Yanagida, M. Yorozu, Y. Okada, K. Takasago, A. Endo, A. Yada, and M. Washio, *J. Applied Phys.* **92**, 1608 (2002)
- [5] H. Tomizawa, H. Dewa, H. Hanaki and F. Matsui, *Quantum Electronics* **37**(8), 697 (2007)
- [6] C. Vicario, A. Ghigo, M. Petrarca, I. Boscolo, S. Cialdi, M. Nicoli, G. Sansone, S. Stagira and C. Vozzi, in *Proc. of EPAC 2004*(Lucerne, Switzerland, 2004), p. 1300
- [7] K.J. Kim, *Nucl. Instr. And Meth.* **A275**, 201 (1989)
- [8] T.Y. Lee, Y.S. Bae, J. Choi, J.Y. Huang, H.S. Kang, M.G. Kim, D.H. Kuk, J.S. Oh, Y.W. Parc, J.H. Park, S.J. Park, and I.S. Ko, *J. Korean Phys. Soc.* **48**, 791 (2006)
- [9] C. Kim, S.J. Park, J.H. Park, Y.W. Parc, J.Y. Huang, J. Choi, and I.S. Ko, *J. Korean Phys. Soc.* **50**, 1427 (2007)
- [10] J. Choi, H. S. Kang, C. M. Lim, J. H. Park, S. J. Park, C. Kim, and I. S. Ko, in *Proc. of Linac 2006* (Knoxville, Tennessee, U.S.A., 2006), p. 112.
- [11] R. Trebino, *Frequency-Resolved Optical Gating: The Measurement of Ultrashort Laser Pulses* (Kluwer Academic Publishers, Boston, 2000), ch.4, pp. 88-89.
- [12] R. Boyd, *Nonlinear Optics*, 2nd ed. (Academic Press, San Diego, 2003), chap. 2, pp. 94-99.